EFFECT OF LOAD MODELING IN COORDINATED ACTIVE POWER CURTAILMENT OF DISTRIBUTED RENEWABLE ENERGY SOURCES

Eleftherios O. Kontis[1], Georgios C. Kryonidis[1], Andreas I. Chrysochos[1], Charis S. Demoulias[1], Grigoris K. Papagiannis[1,*]

[1]School of Electrical and Computer Engineering, Aristotle University of Thessaloniki, Thessaloniki, Greece, GR 54124
**grigoris@eng.auth.gr*

Keywords: Active power curtailment, droop control, sensitivity matrix, voltage-dependent loads, voltage regulation.

Abstract

The increased penetration of distributed renewable energy sources (DRESs) in the existing low-voltage (LV) distribution networks poses a series of technical challenges for distribution system operators (DSOs). Among them, the voltage rise is considered as the most important obstacle that limits the further penetration of DRESs. To increase the installed DRES capacity and to prevent overvoltage issues, active power curtailment (APC) techniques can be applied by the DSOs. A significant drawback of these methods is the non-uniform power curtailment among the installed DRESs. A number of coordinated APC (CAPC) methods have been proposed in the literature to overcome this issue. However, the majority of these techniques model the network loads as constant power loads, thus usually leading to conservative values regarding the power injection of the installed DRESs. In this paper, an enhanced CAPC strategy is presented. Contrary to the conventional approaches, the proposed control scheme employs a more generalized, accurate and realistic representation of power system loads, taking fully into account their voltage-dependent nature. The validity of the developed control strategy is thoroughly investigated using time-series simulations on a radial LV residential network, while its performance is evaluated using appropriate key performance indicators.

1 Introduction

In the last decades, environmental concerns for clean energy and the reduction of carbon emissions as well as the market deregulation and various technological innovations have led to an increased penetration of distributed renewable energy sources (DRESs) in distribution networks. This advent of DRESs has modified drastically the power delivery system from a passive system with downstream unidirectional power flow to an active one with bidirectional power flow. However, it has also posed serious concerns and technical challenges for distribution system operators (DSOs) [1]. Regarding low-voltage (LV) distribution networks, overvoltages are considered as the most substantial problem, leading not only to power quality and reliability issues, but also acting as bottleneck for further integration of DRESs in the distribution grids [2].

For this purpose, various approaches have been proposed to mitigate overvoltages, caused by the high penetration of DRESs. The most promising solutions include grid reinforcement by DSOs, the use of on-load-tap-changer (OLTC) control in medium-/low-voltage transformers, reactive power control and active power curtailment (APC) [3]-[8]. Among them, grid reinforcement is the most straightforward and efficient approach. However, this solution is not commonly preferred by the DSOs due to the high investment costs [4]. The use of OLTC control is also an expensive alternative, since it requires the replacement of the existing transformers with new ones equipped with OLTC [5]. Furthermore, reactive power control, which is extensively used in MV networks [6]-[8], is considered ineffective in LV grids, due to the relatively high R/X ratio of lines and the limited reactive power capability of the grid-interfaced inverters [7], [8].

Due to the mainly resistive nature of LV grids, efficient voltage regulation can be achieved by controlling the active power injection of DRESs [9]. For this purpose, a number of APC techniques have been proposed [10], [11]. Among them, the $P(V)$ droop control (DC) is highly favoured by utilities and prosumers, since it does not require network upgrades or other investments. The principal objective of this control scheme is to mitigate overvoltages by curtailing part of the total injected active power of DRESs. The amount of the curtailed power is calculated with respect to the corresponding voltage at the point of common coupling (PCC). However, a significant drawback of the DC scheme is the non-uniform power curtailment that is mainly observed for DRESs located at distant nodes of radial LV feeders. These prosumers are in a disadvantageous position compared to those located at the beginning of the LV feeders, suffering from higher power curtailment and thus significant loss of revenues.

Citation Information: DOI: 10.1049/cp.2016.1049

To overcome this issue and to guarantee the fairness of power curtailment, a number of coordinated APC (CAPC) techniques, known as fair power sharing (FPS) algorithms, have been proposed in the literature [12], [13]. The main objective of these coordinated control strategies is to uniformly reallocate the active power curtailment among the DRESs of the network, in order to alleviate the high power curtailment of the units located at the end of the feeders. The curtailed power of the installed DRESs is estimated using the sensitivity matrix, based on the simplification that network loads consume constant amount of active power [13]. However, this assumption can be considered as a significant drawback of the method, since it is well-accepted that power system loads are generally voltage-dependent and thus their power is considerably affected by the grid voltage [14], [15].

Scope of this paper is to formulate an enhanced CAPC scheme. Similar to the conventional approaches, the proposed control strategy uses the sensitivity matrix for the estimation of the active power curtailment of DRESs. However, in the proposed approach, the power system loads are modeled in a more generalized and realistic way. For this purpose, the most commonly used static load models, namely the polynomial (or ZIP) model, as well as the exponential load model, are considered and are fully incorporated in the conventional FPS method. The performance of the developed control strategy is thoroughly evaluated using time-series simulations in a radial LV network, while it is also compared with the conventional FPS strategy. Results by both approaches are examined, leading to a better understanding of the impact of load modeling on the voltage profile along the feeder, as well as on the total curtailed power.

2 Theoretical Background

In this section the theoretical background of the DC scheme as well as of the FPS algorithm are briefly presented to provide the appropriate background material.

2.1 Droop Control

The main objective of the DC is to prevent overvoltages by curtailing part of the injected active power [16]. The curtailment depends on the voltage at the PCC and is applied using the droop curve of Fig. 1, which consists of three distinct regions.

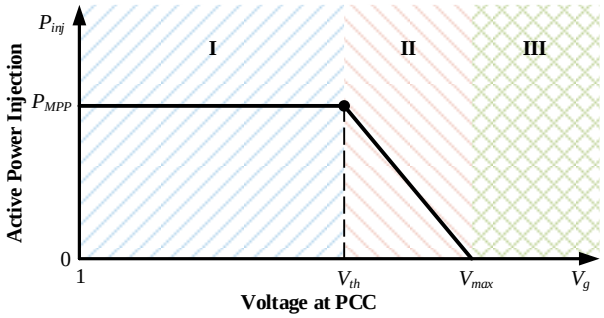

Fig. 1 Typical droop curve

The droop control strategy is expressed mathematically by the following equations:

$$P_{inj} = \begin{cases} P_{MPP}, & V_g \le V_{th} \\ P_{MPP} - P_{MPP}\dfrac{\left(V_g - V_{th}\right)}{\left(V_{max} - V_{th}\right)}, & V_{th} < V_g < V_{max} \\ 0, & V_g \ge V_{max} \end{cases} \quad (1)$$

where V_{th} represents the voltage threshold for the activation of the droop control mechanism, while P_{MPP} stands for the maximum power point (MPP) that the DRES can deliver at a specific time instant. Furthermore, V_g denotes the grid voltage, whereas $V_{\max}$ stands for the maximum voltage threshold. In this paper, $V_{\max}$ is considered equal to the maximum permissible voltage limit of 1.1 p.u., as defined by the EN50160 Standard [17], while V_{th} is set equal to 1.06 p.u. [18].

In the first region of the droop curve, the injected active power P_{inj} is equal to the P_{MPP} value, while the voltage grid remains below the predefined voltage threshold V_{th}. In the second region, the active power curtailment is activated, while in the third region the power injection is set to zero, since the voltage at the PCC exceeds the maximum permissible voltage threshold $V_{\max}$.

The implementation of the DC strategy leads to overvoltage mitigation in LV networks, while it also avoids the repeated tripping of the inverters, based on their ON-OFF operation, which may occur during high generation periods [16]. However, the DC scheme generally results in non-uniform power curtailment among the DRESs installed along the feeder [13].

2.2 The Problem of the Unfair Power Curtailment

The problem of the unfair power curtailment is demonstrated in the radial LV network of Fig. 2. The feeder consists of *n* DRESs and *k* loads, connected to the *m* LV buses. In the general case, each of the *n* DRESs is characterized by its MPP and the actual active power injection P_{inj}, which depends on the voltage at the corresponding PCC. Since the voltage grid V_g^i at each node depends on the grid impedance between the MV/LV transformer and the respective PCC, the

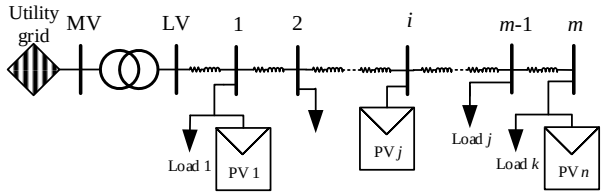

Fig. 2 Simple radial LV feeder

corresponding power injection P_{inj} of each DRES will be also different, resulting in an unfair power curtailment among the installed DRESs. This unfairness can be expressed using the following equations:

$$V_g^1 \neq ... \neq V_g^j \neq V_g^n \tag{2}$$

$$P_{curt}^1 \neq ... \neq P_{curt}^j \neq P_{curt}^n \tag{3}$$

where the absolute curtailed active power P_{curt}^j of each DRES is calculated according to (4).

$$P_{curt}^j = P_{MPP}^j - P_{inj}^j, \forall P_{MPP}^j > P_{inj}^j \tag{4}$$

2.3 Fair Power Sharing Method

The FPS algorithm acts supplementary to the DC mechanism, addressing the unfair power curtailment problem and also maintaining an almost similar voltage profile along the feeder. This is accomplished by properly adjusting the droop characteristics of each DRES. For this purpose, the use of the sensitivity matrix is required, which is an inverse matrix form of the Jacobian matrix [13], [18]. The sensitivity matrix quantifies the impact of the reactive ΔQ and active power variations ΔP on the variation of the voltage magnitude $\Delta|V|$ and angle $\Delta\theta$, as expressed in the following equation:

$$\begin{bmatrix} \Delta\theta \\ \Delta|V| \end{bmatrix} = S \begin{bmatrix} \Delta P \\ \Delta Q \end{bmatrix} = \begin{bmatrix} S_P^\theta & S_Q^\theta \\ S_P^V & S_Q^V \end{bmatrix} \begin{bmatrix} \Delta P \\ \Delta Q \end{bmatrix} \tag{5}$$

Assuming that the change in the reactive power can be neglected during the control period [13], [18], (5) can be simplified to:

$$[\Delta|V|] = [S][\Delta P] = \begin{bmatrix} s_{11} & \cdots & s_{1n} \\ \vdots & \ddots & \vdots \\ s_{n1} & \cdots & s_{nn} \end{bmatrix} [\Delta P] \tag{6}$$

By modelling the network loads as constant power loads and by neglecting their voltage-dependent nature, it can be considered that the voltage variations during the control period are exclusively caused by the changes of the injected active power of the DRESs. Thus, the curtailed active power ΔP_{curt} of the DRES with the minimum P_{MPP} can be calculated using (8), while the active power curtailments $[P_{curt}]$ of the remaining $n-1$ DRESs are computed in a percentage-based fair way by (9):

$$\Delta|V_{\max}| = V_{MPP,i} - V_{DC,i} \tag{7}$$

$$\Delta P_{curt} = \frac{\Delta|V_{\max}|}{\sum_{i=1}^{m} w_i s_{ij}} \tag{8}$$

$$[P_{curt}] = \Delta P_{curt}[w] \tag{9}$$

where i denotes the node with the maximum voltage magnitude after the activation of the droop control, while $V_{MPP,i}$ is the voltage magnitude of the i_{th} node, when all DRESs inject their MPP, and $V_{DC,i}$ is the corresponding voltage provided that the DC is enabled. Note, that (7) is employed to ensure that after the implementation of the FPS algorithm the voltage profile along the feeder will remain almost similar to the one provided by the DC scheme. Moreover, s_{ij} are the corresponding coefficients of the sensitivity matrix, and $[w]$ is a weighting vector related to the MPP conditions defined as:

$$[w] = \frac{[P_{MPP}]}{\min([P_{MPP}])} \tag{10}$$

where $[P_{MPP}]$ is a vector containing the MPPs of all installed DRESs at a given time instant and $\min([P_{MPP}])$ denotes the minimum element of the $[P_{MPP}]$ vector. Finally, the new injection set-points are calculated for each DRES using (4).

To achieve these new injection values, the droop settings of all DRESs must be recalculated, as shown in Fig. 3. Therefore, a power flow calculation is conducted with the new injections P_{inj} to obtain the corresponding network voltages V_{new}. Using the power flow results, a unique pair of voltage and active power injection is created for each DRES (V_{new}^j, P_{inj}^j). The new droop settings are recalculated, depending on which region of the droop characteristic the above pair belongs to. More specifically the following cases are considered:

- $V_{new} < V_{th}$: In this case, the DRES operates in the first region of the droop curve. Thus, P_{MPP}^{new} is considered equal to the corresponding P_{inj}, while V_{th} and $V_{\max}$ remain equal to 1.06 p.u. and 1.1 p.u., respectively.

- $V_{new} > V_{th}$: In this case, the DRES operates in the second region of the droop curve. To recalculate the new droop settings, the following procedure is adopted: $V_{\max}$ remains equal to 1.1 p.u. and the P_{MPP}^{new} is recalculated using (11). In case the computed P_{MPP}^{new} exceeds the MPP that the DRES can deliver, the P_{MPP}^{new} is set equal to P_{MPP} and the V_{th}^{new} is recalculated using (12). Otherwise, V_{th} remains unchanged and equal to 1.06 p.u.

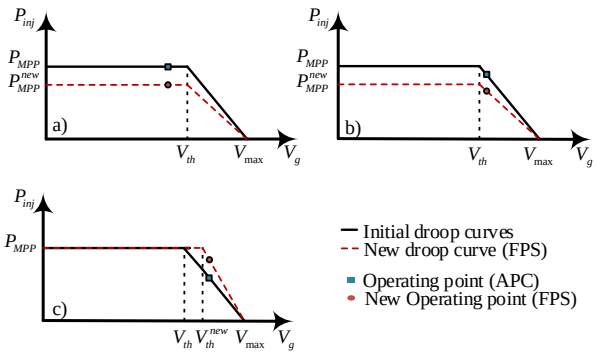

Fig. 3 Reconfiguration of droop curves

$$P_{MPP}^{new} = P_{inj}\frac{V_{th} - V_{\max}}{V_{new} - V_{\max}} \tag{11}$$

$$V_{th}^{new} = V_{\max} + \frac{P_{MPP}^{new}}{P_{inj}}\left(V_{new} - V_{\max}\right) \tag{12}$$

3 Proposed Method

Similar to the conventional FPS algorithm, the proposed control strategy coordinates the droop characteristic of DRESs by exploiting the sensitivity theory. However, contrary to the conventional approach, the proposed method employs a more accurate representation for power system loads, taking also into consideration their voltage-dependent nature. Thus, the curtailed active power of the installed DRESs is calculated with higher accuracy.

3.1 Modelling of Power System Loads

In this paper, the most commonly used by the utilities static load models [19], namely the polynomial and the exponential load model, are considered and incorporated into the conventional FPS algorithm. The polynomial model, referred also as ZIP model, represents the load consumption as a function of the applied voltage, as defined in (13), while the mathematical expression of the exponential model is given in (14):

$$P = P_0\left[Z_p\left(\frac{V_g}{V_0}\right)^2 + I_p\left(\frac{V_g}{V_0}\right) + P_p\right] \tag{13}$$

$$P = P_0\left(\frac{V_g}{V_0}\right)^{n_p} \tag{14}$$

where P is the active power consumption of the load at the operating voltage V_g, while P_0 denotes the rated power of the load at the rated voltage V_0. The parameters of the ZIP model are the coefficients Z_p, I_p, and P_p, which represent the constant impedance, constant current and constant power fraction of the load, respectively. On the other hand, the parameter of the exponential load model is the exponent n_p. Generally, the values of these parameters are determined by the type of the load, e.g. residential, commercial or industrial [14], [15].

The impact of the voltage variation on the active power consumption of the load can be easily estimated by employing the derivatives of (13) and (14) with respect to voltage, as shown in the following equations:

$$\Delta P_{ZIP} = P_0\left[2Z_p\frac{V_g}{V_0^2} + \frac{I_p}{V_0}\right]\Delta V \tag{15}$$

$$\Delta P_{EXP} = \frac{n_p P_0}{V_0^{n_p}} V_g^{(n_p - 1)}\Delta V \tag{16}$$

where ΔV stands for the voltage magnitude variation of the node in which the load is connected.

3.2 Calculation of Active Power Curtailment

Taking into account the voltage-dependent nature of power system loads, the active power variation for each network node can be expressed as:

$$\left[\Delta P\right] = \left[\Delta P_{load}\right] + \left[w\right]\Delta P_{curt} \tag{17}$$

where $\left[\Delta P_{load}\right]$ and $\left[w\right]$ are two vectors of length *m*. The former contains the change in the active power consumption of the installed load at each node, while the latter contains the weighting coefficient for the corresponding DRES. Generally, the elements of the $\left[\Delta P_{load}\right]$ vector can be easily calculated, based on the load model chosen, using (15) and (16), while the coefficient vector is calculated using (10). In case of network nodes without voltage-dependent loads or DRESs, the corresponding elements of vectors $\left[\Delta P_{load}\right]$ and $\left[w\right]$ are set to zero.

The curtailed active power of each DRES can be easily computed by solving the system of linear equations (6), (7) and (17). Eq. (6) linearizes the relation between active power and voltage magnitude in each network node and (7) maintains the voltage profile along the LV feeder. Once the curtailed power is computed, the power injections of all installed DRESs are calculated using (4).

3.3 Actual Implementation

To implement the proposed control strategy, a centralized approach is adopted. A central controller, located at the DSO level, monitors the network operation and calculates the set-points for all installed DRESs at each time instant. The algorithm used for the actual implementation of the proposed control scheme is illustrated in Fig. 4 and consists of 8 main steps, described in detail below:

- **Step-1:** *Initialization phase*. The network configuration is uploaded in the central controller.

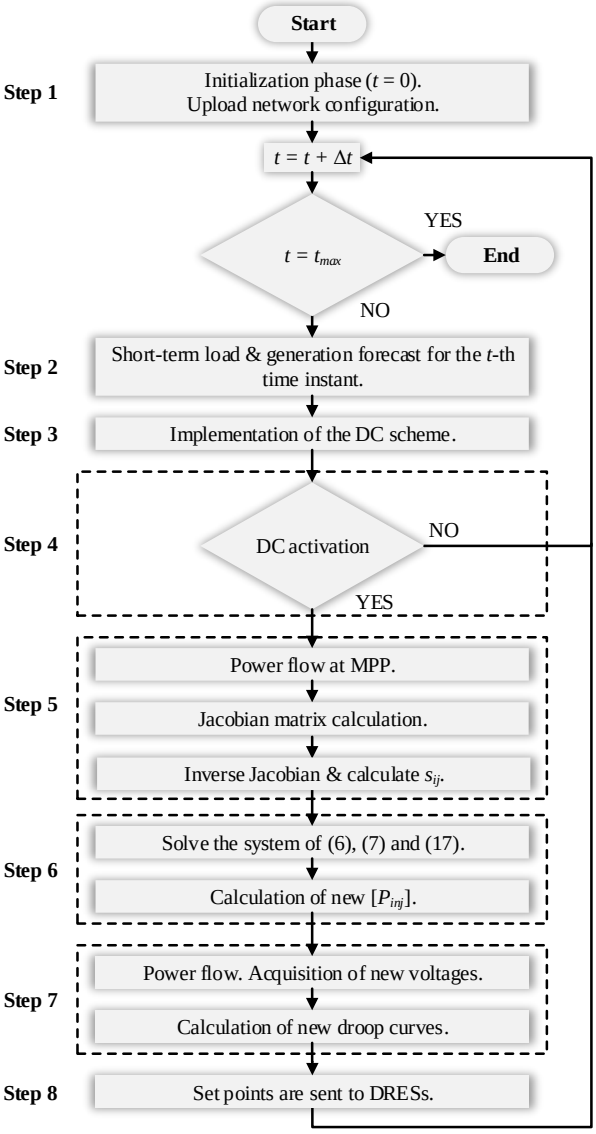

Fig. 4 Actual implementation of the proposed control

- **Step-2:** *Short-term load and generation forecast acquisition*. At each time instant (t), the short-term load and generation forecasts of the next time interval (Δt) are forwarded to the central controller.

- **Step-3:** *Implementation of the DC scheme*. The DC is activated and a simulation is performed using the forecasts of the previous Step.

- **Step-4:** *Check for unfair power curtailment*. The controller evaluates the power flow results of the previous Step and checks if the DC of the installed DRESs is activated. In this case, active power curtailment occurs and the proposed FPS control strategy is enabled. Otherwise, the set-points of all DRESs remain unchanged and the algorithm proceeds to the next time instant.

- **Step-5:** *Calculation of the sensitivity matrix*. A power flow calculation is performed, assuming that all DRESs inject their MPP, as provided from the forecasts of Step 2. Then, the necessary coefficients s_{ij} are computed by inversing the corresponding Jacobian matrix.

- **Step-6:** *Determination of the new injection set-points*. By employing (6), (7) and (17) the central controller determines the curtailed power of each DRES and thus the new active power injections set-points.

- **Step-7:** *Determination of the new droop characteristics*. Using the new injection set-points, a power flow calculation is performed to acquire the new grid voltages. Afterwards, the new droop characteristics are determined, following the procedure discussed in Subsection 2.3.

- **Step-8:** *Dispatch of DRESs*. The new droop characteristics are forwarded to the corresponding DRESs. Then, the procedure moves to the next time instant or terminates if the maximum number of time instants is reached.

4 Simulation Results

In this section, the performance of the proposed FPS control strategy is investigated on a residential LV feeder using time-series simulations. The simulations are performed using the tool of [20].

4.1 System Under Study

The examined residential feeder is presented in Fig. 5. Along this feeder, there are 12 prosumers connected in pair to each network node. Each prosumer has a 3-phase connection to the grid with grounded neutral. The length of the connection wires is considered negligible, while the neutral conductor is grounded at each network node with an impedance of $2+i0.1$ Ω. The line characteristics for the backbone of the network are presented in Table 1. The 20/0.4 kV transformer has a Dyn5 connection and a nominal power of 250 kVA, short circuit voltage of 4%, while the no-load and on-load losses are equal to 325 W and 3250 W, respectively. The voltage in the secondary of the transformer is set to 1.05 p.u. to avoid potential undervoltages during high loading conditions [13]. For sake of simplicity, but with no loss of generality, it is assumed that all houses have the same load characteristics and that they are equipped with identical PV units of 15 kW_p. Regarding the modeling of network loads via (15), a constant impedance representation is chosen.

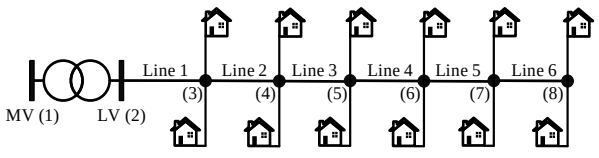

Fig. 5 Residential LV feeder

Table 1 Line characteristics

Line	R_1 (Ω)	X_1 (Ω)	R_0 (Ω)	X_1 (Ω)	C (μF)
#1	0.033	0.003	0.144	0.1476	7.2
#2	0.027	0.002	0.116	0.1189	5.8
#3	0.035	0.003	0.152	0.1558	7.6
#4	0.050	0.004	0.216	0.2214	10.8
#5	0.032	0.003	0.136	0.1394	6.8
#6	0.061	0.005	0.264	0.2706	13.2

4.2. Numerical Results

To thoroughly evaluate the performance of the proposed FPS control strategy, time-series simulations are conducted. The simulation period is considered equal to one day, assuming 15-minute time interval. The generation profile, applied to all installed PVs, is depicted in Fig. 6, while the active and reactive power consumption profiles of each house are illustrated in Fig. 7. Simulation results are presented in Figs. 8 and 9, where the voltage profile along the examined feeder, as well as the power injection during the day in the third and last node of the network are depicted.

As shown in Fig. 8, it is evident that without control (NC case), unacceptable overvoltages are observed during the day. More specifically, in the last three nodes of the network the voltage magnitude is well above the maximum permissible limit of 1.1 p.u. for a long period of time, prohibiting the uninterrupted operation of the

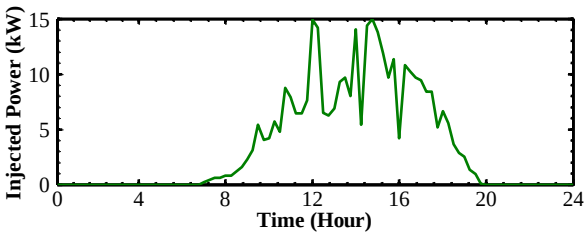

Fig. 6 Active power generation profile

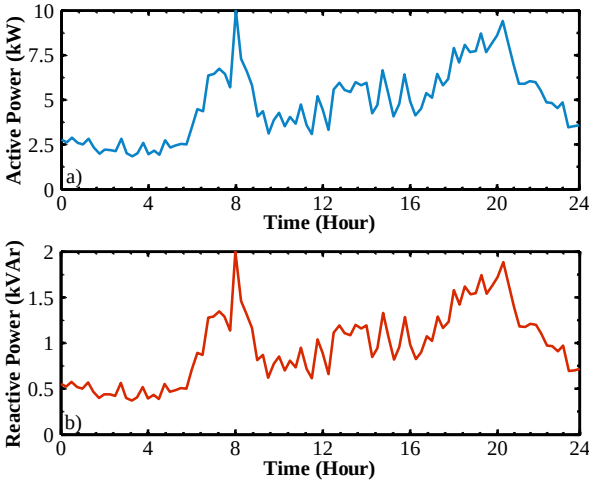

Fig. 7 Power consumption profile. a) Real and b) reactive power

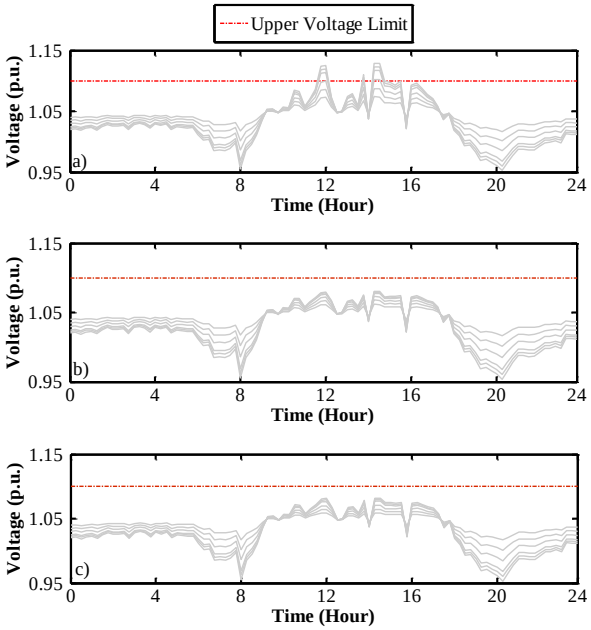

Fig. 8 Voltage profile along the feeder. a) NC, b) DC, and c) PFPS

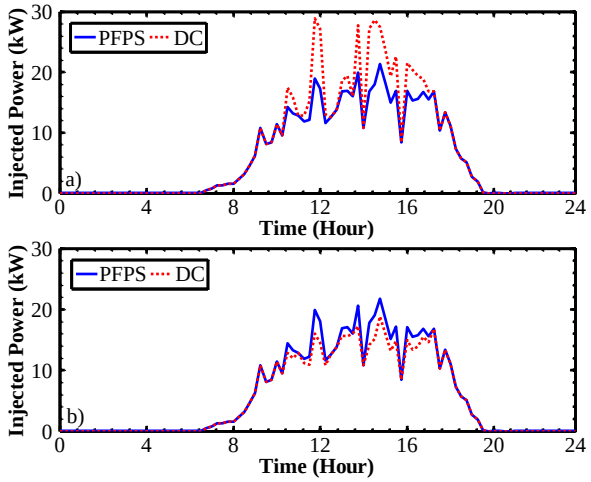

Fig. 9 Active power injection. a) At the third and b) last node of the network

corresponding PV units. On the other hand, the DC control strategy as well as the proposed FPS (PFPS) control scheme are able to mitigate network overvoltages, ensuring the secure and smooth network operation.

Observing Fig. 9, it is clear that the implementation of the DC scheme curtails more power by the prosumers located at the end of the feeder. Indeed, houses located at the third node of the network are able to inject, during the high generation period, up to 28.89 kW of active power. In fact, this injection corresponds almost to 96.3% of the total installed capacity at this specific node. On the contrary, houses located at the most remote network node are able to inject merely 18.79 kW of active power, which corresponds only to 62.63% of the installed capacity. The PFPS control strategy is able to reallocate uniformly the

curtailed active power among the installed PVs, resolving this way the unfair power curtailment issue. To evaluate the uniformity of the active power the key performance indicator (KPI) of (18) is introduced.

$$KPI = \frac{\min\left(\left[P_{inj}(\%)\right]\right)}{\max\left(\left[P_{inj}(\%)\right]\right)} \quad (18)$$

Where $\left[P_{inj}(\%)\right]$ denotes the vector of the normalized injected active power of the PVs to the corresponding MPP. The KPI is calculated for both control strategies on a 15-minute basis and the corresponding average and minimum values are presented in Table 2. Note that a KPI value equal to 1 indicates an ideal uniform active power curtailment among the installed PVs.

The mean value of the proposed KPI factor for the case where only the DC scheme is applied to the PV units is equal to 0.88. Furthermore, the minimum KPI value for this case is merely 0.52. Thus, it is clear that the activation of the DC mechanism results in a highly non-uniform active power curtailment among the PV units. On the other hand, the activation of the PFPS control strategy alleviates the problem, as highlighted by the corresponding results, since the average and the minimum values of the KPI factor are 0.99 and 0.93, respectively.

A second set of time-series simulations is conducted to evaluate the performance of the PFSP control scheme over the conventional FPS (CFPS) method. In these simulations, all networks loads are modelled as constant power loads and the CFPS control strategy is employed to mitigate overvoltages and to uniformly reallocate the curtailment among the PV units. The total curtailed active power of all installed PV units as well as the total captured energy during the day are used to compare the two FPS control schemes and the influence of the different approach in load modeling. More specifically, the total curtailed power for the two implementations is depicted in Fig. 10. The minimum curtailed power is observed for the PFPS control strategy, indicating that the representation of network loads as constant power loads may lead to conservative results, regarding the active power curtailment of the installed PVs. Similar remarks can also be extracted from Table 3, in which the daily total injected energy of all PV units for the two discrete control strategies is presented.

Table 2 Key performance indicator (KPI)

Control Strategy	KPI (value)	
	Mean	Min
DC	0.88	0.52
PFPS	0.99	0.93

Table 3 Daily injected PV energy

Control Strategy	Energy (kWh)
CFPS	820.57
PFPS	848.94

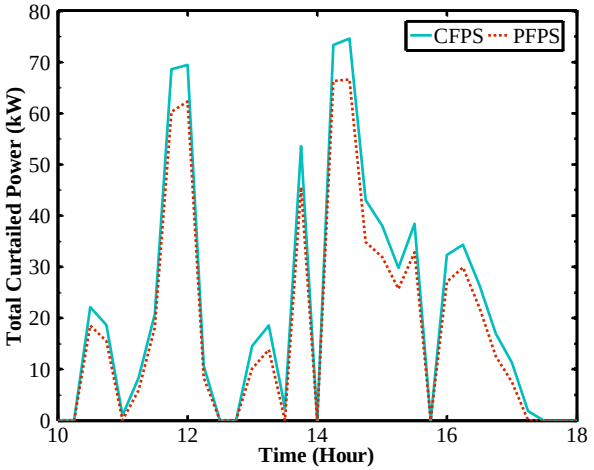

Fig. 10 Total curtailed power for the two distinct implementations of the FPS method

5 Conclusions

In this paper, a coordinated active power curtailment control strategy is presented. The main objectives of the proposed control scheme are to mitigate overvoltages and to ensure a uniform power curtailment among the installed DRESs. The proposed method uses the DC mechanism to tackle overvoltages and reallocates the power curtailment among all DRESs, installed in a feeder, by exploiting the sensitivity matrix. However, contrary to the conventional CAPC schemes, the proposed method employs a more accurate and realistic representation of power system loads. More specifically, the voltage-dependent nature of power system loads is considered and a complete mathematical formulation is presented in order to incorporate the ZIP as well as the exponential load models into the FPS control scheme. From this point of view, the proposed control scheme can be considered as a generalization of the various conventional CAPC techniques.

Time-series simulations in a radial LV residential feeder reveal that the load model, used for the representation of the network loads, may affect considerably the control results, considering the amount of the active power curtailment of the feeder DRESs. Thus, the proposed control method is considered as a valuable tool for the DSOs, since it is offers the capability to incorporate more generalized and accurate load representations into the conventional FPS method. This way, the performance of the FPS control strategy is considerably enhanced and the active power curtailment of the installed DRESs is calculated with significantly higher accuracy.

6 Acknowledgements

This work is supported by the EC-FP7 project “INCREASE” under the Grant Agreement: 608998. Website: http://www.project-increase.eu/.

The work of Georgios C. Kryonidis is supported by the Research Committee of Aristotle University of Thessaloniki via a merit scholarship between 2016 and 2017.

7 References

[1] Walling, R. A. R., Saint, R., Dugan, R. C., Burke, J., Kojovic, L. A.: 'Summary of distributed resources impact on power delivery system', IEEE Trans. Power Deliv., 2008, **23**, (3), pp. 1636–1644

[2] Ueda, Y., Kurokawa, K., Tanabe, T., Kitamura, K., Sugihara, H.: 'Analysis results of output power loss due to the grid voltage rise in grid-connected photovoltaic power generation systems', IEEE Trans. Ind. Electron., 2008, **55**, (7), pp. 2744-2751

[3] Masters, C. L.: 'Voltage rise: The big issue when connecting embedded generation to long 11 kV overhead lines', Power Eng. J., 2002, **16**, pp. 5-12

[4] Kulmala, A., Repo, S., Jrventausta, P.: 'Coordinated voltage control in distribution networks including several distributed energy resources', IEEE Trans. Smart Grid, 2014, **5**, (4), pp. 2010-2020

[5] Elkhatib, M. E., El-Shatshat, R., Salama, M. M. A.: 'Novel coordinated voltage control for smart distribution networks with DG', IEEE Trans. Smart Grid, 2011, **2**, (4), pp. 598–605

[6] Kryonidis, G. C., Demoulias, C. S., Papagiannis, G. K.: 'A nearly decentralized voltage regulation algorithm for loss minimization in radial MV networks with high DG penetration', IEEE Trans. Sustain. Energy, early access

[7] Kabiri, R., Holmes, D. G., McGrath, B. P., Meegahapola, L. G.: 'LV grid voltage regulation using transformer electronic tap changing, with PV inverter reactive power injection', IEEE J. Emerg. Sel. Topics Power Electron., 2015, **3**, (4), pp.1182–1192

[8] Ullah, N. R., Bhattacharya, K., Thiringer, T.: 'Wind farms as reactive power ancillary service providers-technical and economic issues', IEEE Trans. Energy Convers., 2009, **24**, (3), pp. 661–672

[9] Tonkoski, R., Lopes, L. A. C.: 'Voltage regulation in radial distribution feeders with high penetration of photovoltaic'. IEEE Energy 2030, Atlanta, U.S.A., 2008

[10] Alam, M. J. E., Muttaqi, K. M., Sutanto, D.: 'Mitigation of rooftop solar PV impacts and evening peak support by managing available capacity of distributed energy storage systems', IEEE Trans. Power Syst., 2013, **28**, (4), pp. 3874-3884

[11] Brabandere, K. De, Woyte, A., Belmans, R., Nijs, J.: 'Prevention of inverter voltage tripping in high density PV grids'. 19th EU-PVSEC, Paris, France, 2004

[12] Alyami, S., Wang, Y., Wang, C., Zhao, J., Zhao, B.: 'Adaptive real power capping method for fair overvoltage regulation of distribution networks with high penetration of PV systems', IEEE on Trans. Smart Grid, 2014, **5**, (6), pp. 2729-2738

[13] Tonkoski, R., Lopes, L. A. C., El-Fouly, T. H. M.: 'Coordinated active power curtailment of grid connected PV inverters for overvoltage prevention', IEEE Trans. Sustain. Energy, 2011, **2**, (2), pp. 139-147

[14] IEEE Task Force on Load Representation for Dynamic Performance: 'Standard load models for power flow and dynamic performance simulation', IEEE Trans. Power Syst., 1995, **10**, (3), pp. 1302-1313

[15] Hajagos, L. M., Danai, B.: 'Laboratory measurements and models of modern loads and their effect on voltage stability studies', IEEE Trans. Power Syst., 1988, **13**, (2), pp. 584-592

[16] Vandoorn, T. L., De Kooning, J. D. M., Meersman, B., Vandevelde, L.: 'Voltage-based droop control of renewables to avoid on-off oscillations caused by overvoltages', IEEE Trans. Power Del., 2013, **28**, (2), pp. 845–854

[17] EN 50160: 'Voltage characteristics of electricity supplied by public distribution networks', 2010

[18] Ali, M. M. V. M., et al.: 'Fair power curtailment of distributed renewable energy sources to mitigate overvoltages in low-voltage networks'. IEEE Eindhoven PowerTech, Eindhoven, Netherlands, 2015

[19] Milanovic, J., Yamashita, K., Martinez, S., Djokic, S., Korunovic, L.: 'International industry practice on power system load modelling', IEEE Trans. Power Syst., 2013, **28**, (3), pp. 3038-3046

[20] Kryonidis, G. C., et al.: 'A simulation tool for extended distribution grids with controlled distributed generation'. IEEE Eindhoven PowerTech, Eindhoven, Netherlands, 2015